Direct observation of optical magnons in $YBa_2Cu_3O_{6.2}$

D. Reznik* and P. Bourges
Laboratoire Léon Brillouin, CEA, CNRS, CEA-Saclay, 91191 Gif-sur-Yvette, France

H. F. Fong
Department of Physics, Princeton University, Princeton, New Jersey 08544

L. P. Regnault
Département de Recherche Fondamentale sur la Matière Condensée, Service de Physique Statistique, Magnétisme et Supraconductivité, Groupe Magnétisme et Diffraction Neutronique, CEA-Grenoble, 38054 Grenoble, Cedex 9, France

J. Bossy
Institut Laue-Langevin, 38042 Grenoble, Cedex, France

C. Vettier
European Synchrotron Research Facility, Boîte Postale No. 220, 38043 Grenoble, Cedex, France

D. L. Milius and I. A. Aksay
Department of Chemical Engineering, Princeton University, Princeton, New Jersey 08544

B. Keimer
Department of Physics, Princeton University, Princeton, New Jersey 08544
(Received 4 January 1996)

We have used high-energy inelastic neutron scattering to detect optical magnons directly in antiferromagnetic $YBa_2Cu_3O_{6.2}$. The optical magnon gap is 67 ± 5 meV. This implies an intrabilayer superexchange constant perpendicular to the CuO_2 layers of $J_\perp = 0.08 J_\parallel$ where $J_\parallel$ is the in-plane nearest-neighbor superexchange constant. [S0163-1829(96)50222-5]

The unit cell of the high-T_c cuprate $YBa_2Cu_3O_{6+x}$ contains pairs of closely spaced CuO_2 layers, the bilayers, separated by CuO chains. Inelastic neutron scattering experiments have demonstrated that electronic states in different CuO_2 layers belonging to one bilayer are strongly coupled at all doping levels, whereas the coupling across the chains is much weaker.[1–6] The nature of this coupling is well understood only in the antiferromagnetic phase of $YBa_2Cu_3O_{6+x}$, where it results from superexchange interactions between localized spins in the layers. According to several proposed theoretical models, intrabilayer exchange is also responsible for a number of important electronic properties of metallic $YBa_2Cu_3O_{6+x}$, including an enhancement of the superconducting transition temperature T_c as compared to single-layer copper oxide superconductors,[7] and the ''spin pseudogap'' phenomenon in underdoped metallic $YBa_2Cu_3O_{6+x}$.[8] It may also play an important role in the magnetic resonance peak seen in the superconducting state by inelastic neutron scattering, which appears at 40 meV in $YBa_2Cu_3O_7$.[4–6] More generally, the strength of the intrabilayer exchange coupling provides direct information about the energy scales associated with interlayer electron transfer which are an important component of the microscopic description of these materials, and of central importance for some models of high-temperature superconductivity.[9]

Intrabilayer coupling removes the degeneracy between even- and odd-parity electronic states. In the undoped antiferromagnetic phase of $YBa_2Cu_3O_{6+x}$, which in contrast to the superconducting phase is well understood for $x<0.2$, even- and odd-parity electronic excitations correspond to optical and acoustic spin waves, respectively. Neutron scattering experiments[1,5] have shown that the spin dynamics of Cu_2O_4 bilayers in antiferromagnetic $YBa_2Cu_3O_{6+x}$ is well described by the Heisenberg Hamiltonian

$$H = J_\parallel \sum_{n=1,2} \sum_{\langle i,j \rangle} \mathbf{S}_i^n \cdot \mathbf{S}_j^n + J_\perp \sum_i \mathbf{S}_i^1 \cdot \mathbf{S}_i^2, \qquad (1)$$

where $J_\perp$ is the strength of the superexchange coupling between adjacent planes, $J_\parallel$ is the in-plane nearest-neighbor superexchange constant, $\langle i,j \rangle$ is a nearest-neighbor pair within a CuO_2 layer, n is a layer index, and $\mathbf{S}$ are the usual spin operators. Small corrections to Eq. (1) due to exchange anisotropies and interbilayer exchange are important for low-energy acoustic magnons,[1,2,5] but are irrelevant at the high energies under investigation here. Following Ref. 1, diagonalization of the Hamiltonian (1) in spin wave theory results in the magnon dispersions

$$E(\mathbf{q})^2 = (2J_\parallel + \tfrac{1}{2} J_\perp)^2 - (J_\parallel [\cos(q_x a) + \cos(q_y a)] \pm \tfrac{1}{2} J_\perp)^2, \qquad (2)$$

where q_x and q_y are the components of $\mathbf{q}$ and a is the lattice constant. The $+$ sign applies to acoustic magnons, the $-$ sign to optical magnons. These dispersions are shown schematically in Fig. 1. (In our notation $\mathbf{Q}$ represents the wave vector, and $\mathbf{q}$ represents in-plane component of $\mathbf{Q}$ reduced to

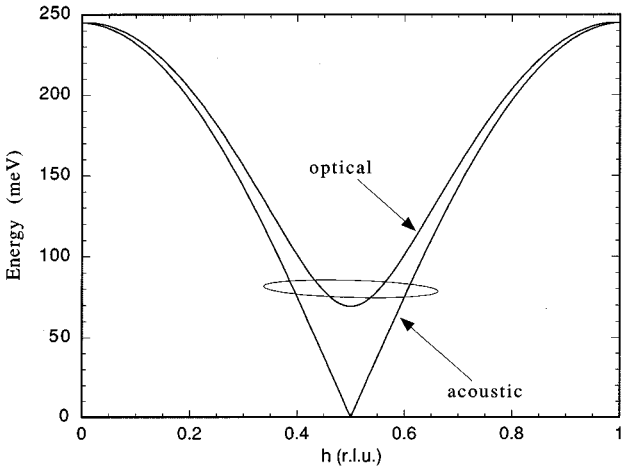

FIG. 1. Schematic diagram of the spin wave dispersions in antiferromagnetic $YBa_2Cu_3O_{6+x}$ in the (hh0) direction ($q_x=(2\pi/a)h$). The superexchange constants used are $J_{\parallel}=120$ meV and $J_{\perp}=10$ meV. Coupling between different bilayers and anisotropy of the in-plane exchange coupling are not included. The ellipse represents the projection of a typical experimental resolution function onto a momentum transfer direction parallel to the CuO_2 layers. The two magnon branches are experimentally resolved according to their different dependence on the momentum transfer perpendicular to the layers which is well outside the experimental resolution.

the first Brillouin zone. The first two indices in our representation of **Q** correspond to the in-plane components in units of $2\pi/a\sim1.63$ Å^{-1}. The third index corresponds to the component perpendicular to the layers in units of $2\pi/c\sim0.53$ Å^{-1}.)

If quantum fluctuations are properly taken into account, the dispersion (2) is modified by a multiplicative renormalization factor Z_c, whose value for the spin-$\frac{1}{2}$ two-dimensional square lattice antiferromagnet is 1.18.[10] To our knowledge a rigorous treatment of the coupled-plane model has not yet been given, although corrections to Z_c due to interlayer coupling are presumably not large for $YBa_2Cu_3O_{6.2}$. Previous neutron work on acoustic magnons[2] has thus been analyzed in terms of an effective $J_{\parallel}=120$ meV which is based on Eq. (2) without quantum renormalization. This value agrees with two-magnon Raman scattering work.[11] For consistency we follow this procedure here and leave a self-consistent treatment of the quantum renormalization factor to future theoretical work.

The minimum energy for optical magnons is thus

$$E_{\mathrm{opt}}=2\sqrt{J_{\perp}J_{\parallel}}. \tag{3}$$

Previous neutron scattering experiments were confined to energies below 60 meV, where only acoustic magnons could be observed. Here we report a direct detection of optical magnons in antiferromagnetic $YBa_2Cu_3O_{6+x}$, which allows us to extract the superexchange constant $J_{\perp}$ via Eq. (3).

Our sample was a large (75 g) single crystal already used in previous neutron experiments.[4,12] The crystal was deoxygenated by keeping it at temperatures between 675 and 750 °C under Ar flow for 10 days. From the temperature dependence of the $\mathbf{Q}=(\frac{1}{2},\frac{1}{2},1)$ magnetic Bragg peak intensity we extracted a Néel temperature of ~390 K. This value of the Néel temperature and careful lattice constants measurements indicate a stoichiometry of $YBa_2Cu_3O_{6.2}$. The experiment was performed on 2T, a double focusing triple axis thermal neutron spectrometer at the ORPHEE reactor at the Laboratoire Léon Brillouin (LLB), and on IN1, a triple axis spectrometer on the hot source at the Institut Laue-Langevin (ILL). Preliminary measurements were also performed on the 1T spectrometer at LLB. On 2T we used copper (111) and (220) monochromators and a graphite analyzer with fixed vertical and horizontal curvature. On IN1 we used vertically curved copper (200) and (220) monochromators and a graphite analyzer with fixed vertical and variable horizontal curvature. On both instruments we used the (002) reflection of the analyzer at final energies of less than 55 meV and the (004) reflection at higher final energies. A contribution from higher-order contamination present at the monochromator on IN1 was eliminated using a nuclear resonance Er filter. A pyrolytic graphite filter in the scattered beam was used in the measurements of Fig. 3. The results obtained on both instruments were in good agreement. In all the measurements on 2T we scanned **Q** while keeping the energy transfer, E, as well as the final energy, E_f, fixed. On IN1 background considerations forced us to perform scans by rocking the sample. In this way we scanned only the direction of **Q**, while keeping its magnitude fixed. Our **q** resolution was insufficient to resolve the positive and negative **q** sides of the dispersion curves because of the broad mosaic of the crystal (see Fig. 1). Counterpropagating spin waves thus appear as a single peak centered at $\mathbf{q}=(\frac{1}{2},\frac{1}{2})$.

Odd-parity (acoustic) and even-parity (optical) magnetic excitations in $YBa_2Cu_3O_{6+x}$ can be distinguished by different dependences of their inelastic neutron scattering cross sections on L (the c-axis component of the momentum transfer **Q**);

$$\left(\frac{\partial^2\sigma}{\partial\Omega\,\partial E}\right)_{\text{odd (acoustic)}}\sim\frac{f^2(\mathbf{Q})\sin^2(\pi z_{\mathrm{Cu}}L)}{E(\mathbf{q})},$$
$$\left(\frac{\partial^2\sigma}{\partial\Omega\,\partial E}\right)_{\text{even (optical)}}\sim\frac{f^2(\mathbf{Q})\cos^2(\pi z_{\mathrm{Cu}}L)}{E(\mathbf{q})}, \tag{4}$$

where $f(\mathbf{Q})$ is the Cu magnetic form factor and $z_{\mathrm{Cu}}=0.28$ is the distance between nearest-neighbor Cu spins within one bilayer expressed as a fraction of the lattice constant c. $E(\mathbf{q})$ is the spin wave energy. The maxima of the acoustic (odd-parity) magnon cross section are at $L=1.75+3.5n$ (n =integer), and the zeroes are at $L=3.5n$. Maxima and zeros are reversed for the optical (even-parity) magnon cross section. The separation of the maxima of the acoustic and optical dynamical structure factors is well outside of our experimental resolution. The observation of magnetic scattering at $L\sim0$, 3.5, 7, . . . , thus automatically implies that it results from optical excitations.

Figures 2 and 3 show the **q** dependence of the scattering cross section at different energies in the vicinity of the two equivalent in-plane antiferromagnetic zone center wave vectors $\mathbf{Q}_{2D}=(\frac{3}{2},\frac{1}{2})$ and $\mathbf{Q}_{2D}=(\frac{1}{2},\frac{1}{2})$. The energy resolution was ~12 meV full width at half maximum (FWHM) for the data in Fig. 2 and ~10 meV FWHM for the data in Fig. 3. In agreement with previous experiments,[2] we observe acoustic magnetic peaks at $\mathbf{Q}=(\frac{3}{2},\frac{1}{2},-1.7)$ and $\mathbf{Q}=(\frac{1}{2},\frac{1}{2},-5.4)$ at 60 meV, while no signal at the positions corresponding to opti-

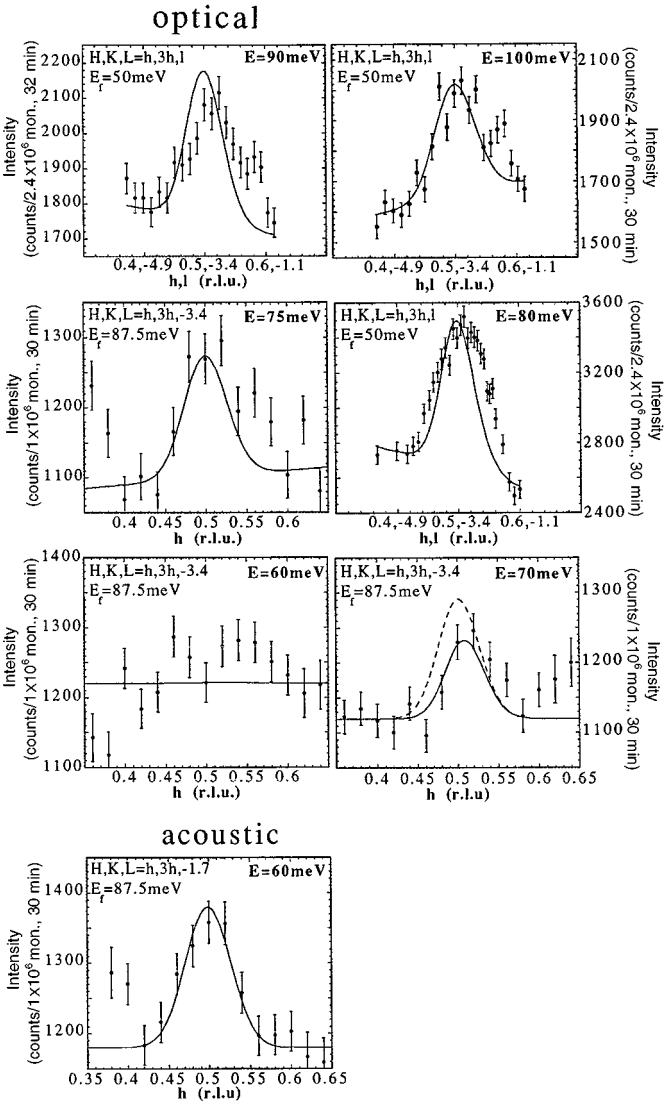

FIG. 2. Magnetic scattering in the vicinity of $\mathbf{Q}_{2D}=(\frac{3}{2},\frac{1}{2})$. 80, 90, and 100 meV spectra were measured on IN1. Note that both h and l are changing in these scans in such a way as to keep **Q** constant. The other spectra were measured on 2T in the (3h,h,0) direction. The solid and dashed lines represent predictions of spin wave theory for $J_\perp=10$ and 9 meV ($E_{\rm opt}=66$ and 69 meV), respectively. The two lines coincide except at 70 meV.

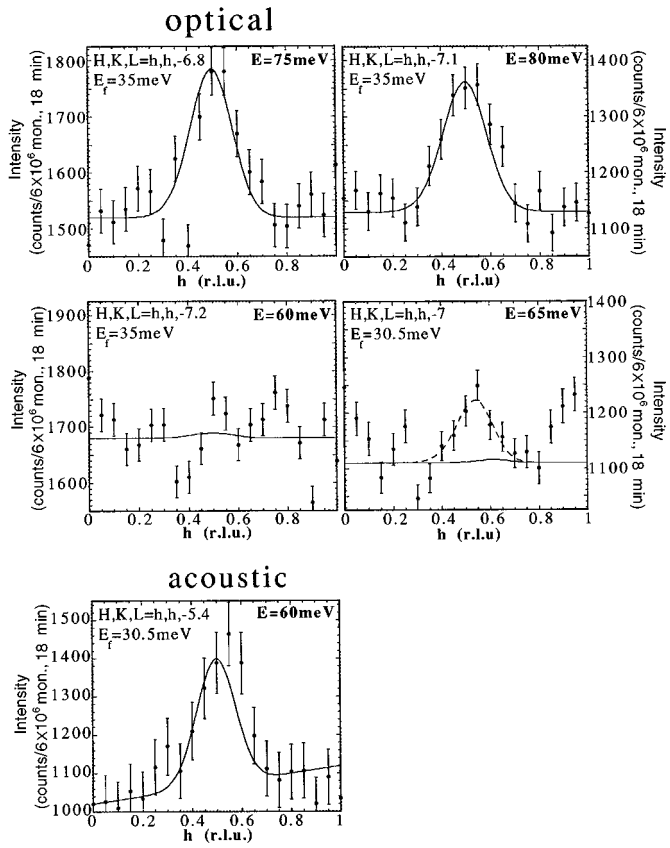

FIG. 3. Magnetic scattering in the vicinity of $\mathbf{Q}_{2D}=(\frac{1}{2},\frac{1}{2})$ measured on 2T. As in Fig. 2 the solid and dashed lines represent predictions of spin wave theory for $J_\perp=10$ and 9 meV ($E_{\rm opt}=66$ and 69 meV) respectively. The two lines coincide except at 65 meV.

cal magnons is visible above the background level. For 75 meV and higher energies, strong optical magnon peaks at $\mathbf{Q}_{2D}=(\frac{3}{2},\frac{1}{2})$ and $\mathbf{Q}_{2D}=(\frac{1}{2},\frac{1}{2})$ are clearly present at both $L=-3.5$ and $L=-7$.

The main difficulties of the experiment arose from spurious contributions due to elastic scattering from the sample and from optical phonon scattering. The spurious contributions were eliminated by a variety of standard methods. Clearly, the reproducibility of our results on two different spectrometers, in two different scattering geometries, and at various different final energies and energy transfers excludes a spurious origin of our observations. As for optical phonon scattering, the maximum phonon energy in $YBa_2Cu_3O_6$ is $\sim$80 meV.[13] We found that data taken at energy transfers of 80 meV and above are unaffected by phonon scattering. Below 75 meV phonon scattering is present and is indeed the major source of the systematic error we quote in the experimental value of $E_{\rm opt}$. Features near the borders of the 65 and 70 meV scans in Figs. 2 and 3, which presumably originate from phonon scattering, make the determination of the magnetic signal intensity less accurate in this energy range. Similar features at small h in the 75 meV scan and the 60 meV acoustic scan in Fig. 2 originate from the contamination by the direct beam at low angles. We also cannot definitively rule out a lattice vibrational contribution to the small signal detected at $\mathbf{q}=(\frac{1}{2},\frac{1}{2})$ and 65 meV. However, at 60 meV there is no peak near $\mathbf{q}=(\frac{1}{2},\frac{1}{2})$, and the upper bound on the optical magnon intensity is much smaller than the acoustic magnon intensity at the same energy, in agreement with the previous measurements.[2]

We have compared the experimental data with predictions of the spin wave theory for $J_\parallel=120$ meV and two values of $J_\perp$, 9 and 10 meV, which correspond to $E_{\rm opt}\sim$66 and 69 meV, respectively. The lines in Figs. 2 and 3 represent the results of numerical convolutions of the theoretically predicted spin wave cross section [Eqs. (2) and (4)] with the experimental resolution function. Data taken at different **Q** were adjusted for the magnetic form factor $f(\mathbf{Q})$ whose functional form was taken from Refs. 2 and 14. The *only* adjustable parameters in this comparison are a *single* overall scale factor and a linear background which was adjusted for each of the figures separately to achieve good agreement with the data. The agreement of the data with the theoretical prediction is obviously excellent, except for some systematic de-

viations of the theoretical curves from the data in the high-energy scans of Fig. 2. These scans were taken by rocking the sample and are therefore particularly sensitive to the multidomain mosaic structure of our crystal, which did not enter into our calculation.

The theoretical line shapes for both values of $J_\perp$ were significantly different only for energies close to $E_{\rm opt}$. $J_\perp<9$ meV results in too much intensity at 60 meV, and $J_\perp>10$ meV results in too little intensity at 70 and 75 meV as compared to the data. A more accurate determination of $E_{\rm opt}$ and $J_\perp$ depends on the origin of the small signal at $\mathbf{q}=(\frac{1}{2},\frac{1}{2})$ and 65 meV, and on the precise shape of the background at 65 and 70 meV. At this point we can conclude that $65\lesssim E_{\rm opt}\lesssim 70$ meV, which gives $J_\perp=0.08J_\parallel\sim 10$ meV.[15] A more precise determination requires further investigation.

Our results provide an energy scale for even-parity magnetic excitations in $YBa_2Cu_3O_{6+x}$. According to previous neutron scattering experiments, even- and odd-parity components of the dynamical susceptibility are not degenerate even in the doped systems. Odd-parity excitations with similar **Q** dependence to acoustic spin waves, but with suppressed low-energy weight and anomalous temperature dependence have been observed in underdoped superconducting $YBa_2Cu_3O_{6+x}$ $(0.4<x<0.94)$.[3,5,6] The magnetic resonance peak in the superconducting state at high oxygen concentrations also follows the odd structure factor in Eq. (4).[4,5,6,16] Even-parity excitations have thus far not been observed in the metallic or superconducting states of $YBa_2Cu_3O_{6+x}$.

In many microscopic models, $J_\perp$ retains a well-defined meaning in the metallic phase, and its influence on the physical properties of bilayer superconductors has been the focus on much theoretical work.[7] Our experimental value agrees well with recent band-theory calculations which predict that $J_\perp\sim 13$ meV.[17] A conclusion which is rather independent of specific models is that the exchange integral is proportional to the square of the overlap of the atomic wave functions. The ratio $J_\perp/J_\parallel=0.08$ thus implies a ratio of $t_\perp/t_\parallel\sim\sqrt{0.08}=0.28$ between the hopping matrix elements, a fundamental parameter that must enter into all microscopic models of bilayer superconductors. According to band theory, the value of $t_\perp$ implied by our experiment should result in a substantial splitting between bonding and antibonding bands which is not observed in photoemission experiments on some bilayer compounds.[18]

In summary, our measurements of the optical magnon branch in $YBa_2Cu_3O_{6.2}$ show that the minimum optical magnon energy is between 65 and 70 meV, and $J_\perp\sim 10$ meV. It is important to extend these measurements to the doped phases.

We thank B. Roessli, J. Kulda, and P. Palleau for assistance with the measurements at the ILL, M. Braden and B. Hennion for assistance with measurements at LLB, and P. W. Anderson and A. J. Millis for helpful discussions. The work at Princeton University was supported by the MRSEC Program of the National Science Foundation under Grant No. DMR-9400362, and by the Packard Foundation. We also acknowledge the European ''Human Capital and Mobility'' program No. ERBCHRXCT930113 for financial support.

*Current address: Department of Physics, University of California, San Diego, La Jolla, CA 92093-0319.

[1] J. M. Tranquada, G. Shirane, B. Keimer, S. Shamoto, and M. Sato, Phys. Rev. B **40**, 4503 (1989).

[2] S. Shamoto, M. Sato, J. M. Tranquada, B. Sternlieb, and G. Shirane, Phys. Rev. B **48**, 13 817 (1993).

[3] J. M. Tranquada, P. M. Gehring, G. Shirane, S. Shamoto, and M. Sato, Phys. Rev. B **46**, 5561 (1992).

[4] H. F. Fong, B. Keimer, P. W. Anderson, D. Reznik, F. Dogan, and I. A. Aksay, Phys. Rev. Lett. **75**, 316 (1995).

[5] J. Rossat-Mignot, L. P. Regnault, P. Bourges, P. Burlet, C. Vettier, and J. Y. Henry, in *Selected Topics in Superconductivity* (World Scientific, Singapore, 1993), p. 265.

[6] J. Rossat-Mignot, L. P. Regnault, C. Vettier, P. Bourges, P. Burlet, J. Bossy, J. Y. Henry, and G. Lapertot, Physica C **185-189**, 86 (1991); P. Bourges, L. P. Regnault, Y. Sidis, and C. Vettier, Phys. Rev. B **53**, 876 (1996).

[7] See, e.g., I. I. Mazin and V. M. Yakovenko, Phys. Rev. Lett. **75**, 4134 (1995), and references therein.

[8] A. J. Millis and H. Monien, Phys. Rev. B **50**, 16 606 (1994), and references therein.

[9] S. Chakravarty, A. Sudbo, P. W. Anderson, and S. Strong, Science **261**, 337 (1993), and references therein.

[10] E. Manousakis, Rev. Mod. Phys. **63**, 1 (1991), and references therein.

[11] R. R. Singh, P. A. Fleury, K. B. Lyons, and P. E. Sulewski, Phys. Rev. Lett. **62**, 2736 (1989).

[12] D. Reznik, B. Keimer, F. Dogan, and I. A. Aksay, Phys. Rev. Lett. **75**, 2396 (1995).

[13] L. Pintschovius, N. Pyka, W. Reichardt, A. Yu Rumiantsev, N. L. Mitrofanov, A. S. Ivanov, G. Collin, and P. Bourges, Physica B **174**, 323 (1991).

[14] H. Casalta, P. Schleger, E. Brecht, W. Moontfrooij, N. H. Anderson, B. Lebech, W. W. Schmahl, H. Fuess, R. Liang, W. N. Hardy, and T. Wolf, Phys. Rev. B **50**, 9688 (1994).

[15] Note that if $Z_c=1.18$ is included in Eq. (2) and the unrenormalized $J_\parallel=100$ meV is used, the resulting ratio $J_\perp/J_\parallel=0.08$ is almost identical. A more accurate treatment using Schwinger bosons gives $J_\perp\sim 14$ meV. We thank A. J. Millis for pointing this out to us.

[16] H. A. Mook, M. Yethiraj, G. Aeppli, T. E. Mason, and T. Armstrong, Phys. Rev. Lett. **75**, 3490 (1993).

[17] O. K. Anderson, A. I. Liechtenstein, O. Jepsen, and F. Paulsen, J. Phys. Chem. Solids **56**, 1573 (1995).

[18] H. Ding *et al.*, Phys. Rev. Lett. **76**, 1533 (1996); P. W. Anderson, Science **256**, 1526 (1992). ,